Article

Formation of Spectral Intermediate G#C and A#T Anion Complex in Duplex DNA Studied by Pulse Radiolysis

Ryuhei Yamagami, Kazuo Kobayashi, and Seiichi Tagawa

J. Am. Chem. Soc., **2008**, 130 (44), 14772-14777 • DOI: 10.1021/ja805127e • Publication Date (Web): 09 October 2008

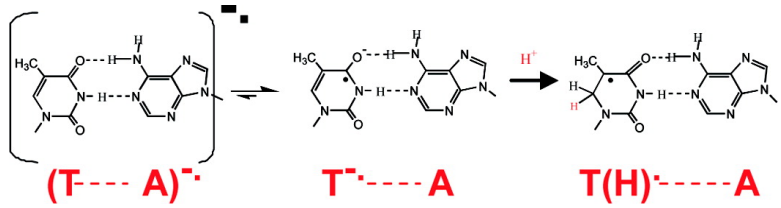

More About This Article

Additional resources and features associated with this article are available within the HTML version:

- Supporting Information
- Access to high resolution figures
- Links to articles and content related to this article
- Copyright permission to reproduce figures and/or text from this article

View the Full Text HTML

J|A|C|S
ARTICLES

Published on Web 10/09/2008

Formation of Spectral Intermediate G−C and A−T Anion Complex in Duplex DNA Studied by Pulse Radiolysis

Ryuhei Yamagami, Kazuo Kobayashi,* and Seiichi Tagawa*

The Institute of Scientific and Industrial Research, Osaka University, Mihogaoka 8-1, Ibaraki Osaka 567-0047, Japan

Received July 13, 2008; E-mail: kobayasi@sanken-osaka.u.ac.jp; tagawa@sanken.osaka-u.ac.jp

Abstract: The dynamics of electron adducts of 2′-deoxynucleotides and oligonucelotides (ODNs) were measured spectroscopically by nanosecond pulse radiolysis. The radical anions of the nucleotides were produced within 10 ns by the reaction of hydrated electrons (e_{aq}^-) and were protonated to form the corresponding neutral radicals. At pH 7.0, the radical anion of deoxythymidine ($dT^{\bullet-}$) was protonated to form the neutral radical $dT(H)^{\bullet}$ in the time range of microseconds. The rate constant for the protonation was determined as 1.8×10^{10} M^{-1} s^{-1}. In contrast, the neutral radical of $dC(H)^{\bullet}$ was formed immediately after the pulse, suggesting that the protonation occurs within 10 ns. The transient spectra of excess electrons of the double-stranded ODNs 5′-TAATTTAATAT-3′ (**AT**) and 5′-CGGCCCGGCGC-3′ (**GC**) differed from those of pyrimidine radicals (C and T) and their composite. In contrast, the spectra of the electron adducts of the single-stranded ODNs **GC** and **AT** exhibited characteristics of C and T, respectively. These results suggest that, in duplex ODNs, the spectral intermediates of G−C and A−T anions complex were formed. On the microsecond time scale, the subsequent changes in absorbance of the ODN **AT** had a first-order rate constant of 4×10^4 s^{-1}, reflecting the protonation of T.

Introduction

In the early stages of radiation-induced DNA damage, high-energy radiation ionizes the nucleic acid bases, generating positive holes and electrons within the DNA strand.[1−3] Identification of the DNA sites that trap these holes and electrons is essential to understanding the progression of radiation-induced damage. The positive holes migrate to guanine (G) sites,[4] which have the lowest oxidation potential among the four bases. The cationic radicals of G participate in further irreversible reactions, which may lead to oxidative DNA damage.[5] Less is known, however, about the complementary excess electrons, with most of the knowledge of their behavior coming from ESR studies of γ-irradiated frozen solutions of DNA.[2,6−8] These studies revealed that when DNA was irradiated at <77 K, cytosine (C) was the primary site for trapping excess electrons.[6−8] At annealing temperatures, the irreversible protonation of $T^{\bullet-}$ competes with electron tunneling[6c,d,7c] and acts as a stable trapping site for reductive damage caused by the formation of the 5,6-dihydrothymine 5-yl radical.[6e] In contrast, protonation of $C^{\bullet-}$ is reversible and electron transfer proceeds as the thermal activation process which involves $C^{\bullet-}$ as the intermediate electron carrier.[1,6f,9]

Excess electrons have recently been shown to migrate through duplex DNA by a hopping mechanism, in which the pyrimidine bases $T^{\bullet-}$ and $C^{\bullet-}$ act as intermediates.[10−12] During this process,

(1) Steenken, S. *Biol. Chem.* **1997**, *378*, 1293–1297.
(2) Bernhard, W. A.; Close, D. M. In *Charged Particles and Photon Interactions with Matter*; Mozunder, A., Hatano, Y., Eds.; Marcel Dekker, Inc: New York, Basel, 2004; p 431.
(3) Cai, Z.; Sevilla, M. D. In *Long Charge Transfer in DNA II*; Schuster, G. B., Ed; Topics in Current Chemistry; Springer: Berlin, 2004; p 103, *237*.
(4) (a) Giese, B. *Acc. Chem. Res.* **2000**, *33*, 631–636. (b) Schuster, B. G. *Acc. Chem. Res.* **2000**, *33*, 253–260. (c) Becker, D.; Sevilla, M. D. *Electron Paramagnetic Resonance*; The Royal Society of Chemistry: Cambridge, 1998; p 79. (d) Lewis, F. D.; Letsinger, R. L.; Wasielewski, M. R. *Acc. Chem. Res.* **2001**, *34*, 159–170. (f) Takada, T.; Kawai, K.; Fujitsuka, M.; Majima, T. *Proc. Natl. Acad. Sci. U.S.A.* **2004**, *101*, 14002–14006.
(5) (a) Kasai, H.; Yamaizumi, Z.; Berger, M.; Cadet, J. *J. Am. Chem. Soc.* **1992**, *114*, 9692–9694. (b) Burrows, C. J.; Muller, J. G. *Chem. Rev.* **1998**, *98*, 1109–1152. (c) Cadet, J.; Douki, T.; Gasparutto, D.; Ravanat, J.-L. *Mutat. Res.* **2003**, *531*, 5–23. (d) Misiaszek, M.; Crean, C.; Joffe, A.; Geacintov, N. E.; Shafirovich, V. *J. Biol. Chem.* **2004**, *279*, 32106–32115. (e) Kino, K.; Saito, I.; Sugiyama, H. *J. Am. Chem. Soc.* **1998**, *120*, 7373–7374. (f) Nakatani, K.; Dohno, C.; Saito, I. *J. Am. Chem. Soc.* **2001**, *123*, 9681–9682. (g) Lee, Y. A.; Yun, B. H.; Kim, S. K.; Margolin, Y.; Dedon, P. C.; Geacintov, N. E.; Shafirovich, V. *Chem.—Eur. J.* **2007**, *13*, 4571–4581. (h) Crean, C.; Uvaydov, Y.; Geacintov, N. E.; Shafirovich, V. *Nucleic Acids Res.* **2008**, *36*, 742–755.
(6) (a) Yan, M.; Becker, D.; Summerfield, S.; Renke, P.; Sevilla, M. D. *J. Phys. Chem.* **1992**, *96*, 1983–1989. (b) Cai, Z.; Li, X.; Sevilla, M. D. *J. Phys. Chem. B* **2002**, *106*, 2755–2762. (c) Razskazovkii, Y.; Swarts, S. G.; Falcone, J. M.; Taylor, C.; Sevilla, M. D. *J. Phys. Chem. B* **1997**, *101*, 1460–1467. (d) Cai, Z.; Gu, Z.; Sevilla, M. D. *J. Phys. Chem. B* **2000**, *104*, 10406–10411. (e) Wang, W.; Sevilla, M. D. *Radiat. Res.* **1994**, *138*, 9–17. (f) Li, X.; Cai, Z.; Sevilla, M. D. *J. Phys. Chem. B* **2001**, *105*, 10115–10123.
(7) (a) Bernhard, W. A. *J. Phys. Chem.* **1989**, *93*, 2187–2189. (b) Debije, M. G.; Bernhard, W. A. *J. Phys. Chem. A* **2002**, *106*, 4608–4615. (c) Debije, M. G.; Milano, M. T.; Bernhard, W. A. *Angew. Chem., Int. Ed.* **1999**, *38*, 2752–2756. (d) Debije, M. G.; Bernhard, W. A. *J. Phys. Chem. B* **2000**, *104*, 7845–7851.
(8) Cullius, P. M.; Evans, P.; Malone, M. E. *Chem. Commun.* **1996**, 985–986.
(9) Steenken, S. *Free Radical Res. Commun.* **1992**, *16*, 349–379.
(10) (a) Behrens, C.; Burgdorf, L. T.; Schwgler, A.; Carell, T. *Angew. Chem., Int. Ed.* **2002**, *41*, 1763–1766. (b) Behrens, C.; Ober, M.; Carell, T. *Eur. J. Org. Chem.* **2002**, 3281–3289. (c) Behrens, C.; Carell, T. *Chem. Commun.* **2003**, 1632–1633. (d) Breeger, S.; Hennecke, U.; Carell, T. *J. Am. Chem. Soc.* **2004**, *126*, 1302–1303. (e) Manetto, A.; Beeger, S. *Angew. Chem., Int. Ed.* **2006**, *45*, 318–321.

10.1021/ja805127e CCC: $40.75

G−C, but not A−T, base pairs reduce the efficiency of electron transfer. Using pyrene-modified nucleosides as model compounds, interference with electron migration was found to be due to protonation of $C^{\bullet -}$.[13] However, protonation of $T^{\bullet -}$ and $C^{\bullet -}$ in DNA at room temperature has not been observed directly.

Radiation-induced DNA damage results not only from the primary impact of high energy quanta but also from secondary particles generated during the ionization process. Recent experimental and theoretical studies have shown that even very low energy electrons may induce strand breaks in DNA.[14] This process can occur via several pathways, including dissociative electron attachment, in which electrons formed as secondary products of radiation bind to nucleobases and cause bonds to break. Thus, knowledge of the distribution of excess electron sites and of reliable electron affinities for DNA is of great importance.

The energetics and structures of radical anion states of nucleobases and their complexes have been studied intensively by theoretical methods.[15−18] The electron affinities of 2′-deoxyribonucleosides, as determined by theoretical calculations, range from 0.44 to 0.06 eV and are in the order dT > dC > dG ≈ dA. In a solution of dichloromethanone, however, the reduction potential of C is lowered by base pairing with G.[19] The situation in DNA likely differs significantly from that of isolated nucleosides. The electron adduct nucleobases may be affected by the interaction fields caused by base pairing and base stacking, as observed in cation radicals of G in DNA.[20,21]

Table 1. Sequences of the Oligonucleotides Examined in This Work

name	sequence (5′→3′)
AT	5′ TAATTTAATAT 3′
	3′ ATTAAATTATA 5′
Pal AT	5′ ATAATTTAAATTAT 3′
	3′ TATTAAATTTAATA 5′
GC	5′ CGGCCCGGCGC 3′
	3′ GCCGGGCCGCG 5′
Pal GC	5′ GCGGCCCGGGCCGC 3′
	3′ CGCCGGGCCCGGCG 5′

In duplex DNA, excess electrons of nucleobases can be generated by pulse radiolysis of a deaerated aqueous solution. Hydrated electrons (e_{aq}^-) can react with all four nucleobases, and the resulting products of the nucleic acids have been identified spectroscopically.[22−24] This paper describes the use of nanosecond pulse radiolysis to investigate the dynamics of excess electrons in duplex DNA. Differences in the dynamics of ODNs and corresponding isolated nucleotides are reported.

Experimental Section

Materials. ODNs (Table 1) were synthesized at Sigma Genosis Biotech Co., Ltd., Japan, dissolved in 20 mM sodium phosphate buffer (pH 7.0), and the two strands were annealed by heating the samples to 90 °C for 5 min and allowing the samples to cool slowly to room temperature over 1 h. The formation of double-stranded ODNs was confirmed by monitoring absorbance at 260 nm. All other reagents were of the highest purity available commercially.

Pulse Radiolysis. Samples for pulse radiolysis were prepared by deoxygenating aqueous solutions of double-stranded ODNs (0.5−2 mM) or deoxynucleotides (5−150 mM) in 20 mM sodium phosphate buffer containing 0.1 M *tert*-butyl alcohol (for scavenging OH radicals) in sealed cells and flushing with argon. Pulse radiolysis experiments were performed with a linear accelerator at the Institute of Scientific and Industrial Research, Osaka University.[25−27] The pulse width and pulse energy were 8 ns and 27 MeV, respectively. The light source was a Xe flash lamp (a continuous spectrum from 300 to 1600 nm). The analyzing light was monitored with a Ritsu MC-10N monochromator and detected by PIN Si (Hamamatsu S1722) or InGaAs (Hamamatsu G3476) photodiodes. The signals were corrected using a Sony/Tektronics SCD transient digitizer. For time-resolved transient absorption spectral measurements, the monitored light was focused into a quartz optical fiber, which

(11) (a) Ito, T.; Rokita, S. E. *J. Am. Chem. Soc.* **2003**, *125*, 11480–11481. (b) Ito, T.; Rokita, S. E. *Angew. Chem., Int. Ed.* **2004**, *43*, 1839–1842. (c) Ito, T.; Rokita, S. E. *J. Am. Chem. Soc.* **2004**, *126*, 15552–15559.

(12) (a) Wagenknecht, H.-A. *Angew. Chem., Int. Ed.* **2003**, *42*, 2454–2460. (b) Kaden, P.; Mayer-Enthart, E.; Trifonov, A.; Fiebig, T.; Wagenknecht, H.-A. *Angew. Chem., Int. Ed.* **2005**, *44*, 1636–1639. (d) Wagner, C.; Wagenknecht, H.-A. *Chem.—Eur. J.* **2005**, *11*, 1871–1876.

(13) (a) Huber, R; Fiebig, T.; Wagenknecht, H. A. *Chem. Commun.* **2003**, 1878–1879. (b) Raytchev, M.; Mayer, E.; Amann, N.; Wagenknecht, H.-A.; Fiebig, T. *Chem. Phys. Chem.* **2004**, *5*, 706–712.

(14) (a) Boudaiffa, B.; Cloutier, P.; Hunting, D.; Huels, M. A.; Sanche, L. *Science* **2000**, *287*, 1658. (b) Pan, X.; Cloutier, P.; Hunting, D.; Sanche, L. *Phys. Rev. Lett.* **2003**, *90*, 208102. (c) Caron, L. G.; Sanche, L. *Phys. Rev. Lett.* **2003**, *91*, 113201. (d) Zheng, Y.; Cloutier, P.; Hunting, D.; Wagner, J. R.; Sanche, L. *J. Am. Chem. Soc.* **2004**, *126*, 1002–1003. (e) Abdoul-Carme, H.; Huels, M. A.; Sanche, L. *J. Am. Chem. Soc.* **2001**, *123*, 5354–5355. (f) Huels, M. A.; Boudaiffa, B.; Cloutier, P.; Hunting, D.; Sanche, L. *J. Am. Chem. Soc.* **2003**, *125*, 4467–4477. (g) Kumar, A.; Sevilla, M. D. *J. Am. Chem. Soc.* **2008**, *130*, 2130–2131. (h) Li, X.; Sevilla, M. D.; Sanche, L. *J. Am. Chem. Soc.* **2003**, *125*, 13668–13669. (i) Barros, R.; Skurski, P.; Simons, J. *J. Phys. Chem. B* **2002**, *106*, 7991–7994.

(15) Colson, A.-O.; Besler, B.; Sevilla, M. D. *J. Phys. Chem.* **1992**, *96*, 9787–9794.

(16) (a) Kim, S.; Schaefer, H. F., III. *J. Chem. Phys.* **2007**, *126*, 64301–64309. (b) Zhang, J. D.; Xie, Y.; Shaefer, H. F., III. *J. Phys. Chem. A* **2006**, *110*, 12010–12016. (c) Richarardson, N. A.; Wesolowski, S. S.; Shaefer, H. F., III. *J. Phys. Chem. B* **2003**, *107*, 848–853. (d) Kumar, A.; Knapp-Mohammady, M.; Mishra, P. C.; Suhai, S. *J. Comput. Chem.* **2004**, *25*, 1047–1059. (e) Richarardson, N. A.; Wesolowski, S. S.; Shaefer, H. F., III. *J. Am. Chem. Soc.* **2002**, *124*, 10163–10170. (f) Richardson, N. A.; Gu, J.; Wang, S.; Yaoming, X.; Shaefer, H. F., III. *J. Am. Chem. Soc.* **2004**, *126*, 4404–4411. (g) Gu, J.; Xie, Y.; Shaefer, H. F., III. *J. Phys. Chem. B* **2005**, *109*, 13067–13075.

(17) Blancafort, L.; Voityuk, A. A. *J. Phys. Chem. A* **2007**, *111*, 4714–4717.

(18) (a) Seidel, C. A. M.; Schulz, A.; Sauer, M. H. M. *J. Phys. Chem.* **1996**, *100*, 5541–5553. (b) Steenken, S.; Telo, J. P.; Novais, H. M.; Candeias, L. P. *J. Am. Chem. Soc.* **1992**, *114*, 4701–4709. (c) Wiley, J. R.; Robinson, J. M.; Ehdaie, S.; Chen, E. C. M.; Chen, E. S. D. *Biochem. Biophys. Res. Commun.* **1991**, *31*, 841–845.

(19) Kawai, K.; Yokoohji, A.; Tojo, S.; Majima, T. *Chem. Commun.* **2003**, 2840–2841.

(20) (a) Saito, I.; Nakamura, T.; Nakatani, K.; Yoshioka, Y.; Yamaguchi, K.; Sugiyama, H. *J. Am. Chem. Soc.* **1998**, *120*, 12686–12687. (b) Yoshioka, Y.; Kitagawa, Y.; Takano, Y.; Yamaguchi, K.; Nakamura, T.; Saito, I. *J. Am. Chem. Soc.* **1999**, *121*, 8712–8719.

(21) Kobayashi, K.; Yamagami, R.; Tagawa, S. *J. Phys. Chem. B* **2008**, *112*, 10752–10757.

(22) Steenken, S.; Telo, J. P.; Novais, H. M.; Candeias, L. P. J. *J. Am. Chem. Soc.* **1992**, *114*, 4701–4709.

(23) Moorthy, P. N.; Hayon, E. *J. Am. Chem. Soc.* **1975**, *97*, 3345–3350.

(24) Visscher, K. J.; Hom, M.; Loman, H.; Spoelder, H. J. W.; Verberne, J. B. *Radiat. Phys. Chem.* **1988**, *32*, 465–473.

(25) Kobayashi, K.; Tagawa, S. *J. Am. Chem. Soc.* **2003**, *125*, 10213–10218.

(26) (a) Kobayashi, K.; Hayashi, K. *J. Am. Chem. Soc.* **1990**, *112*, 6051–6053. (b) Suzuki, S.; Kohzuma, T.; Deligeer; Yamaguchi, K.; Nakamura, N.; Shidara, S.; Kobayashi, K.; Tagawa, S *J. Am. Chem. Soc.* **1994**, *116*, 11145–1146. (c) Kobayashi, K.; Tagawa, S.; Daff, S.; Sagami, I; Shimizu, T. *J. Biol. Chem.* **2001**, *276*, 39864–39871. (d) Kobayashi, K.; Mostafa, G.; Tagawa, S.; Yamada, M. *Biochemistry* **2005**, *44*, 13567–13572. (e) Mustafa, G.; Ishikawa, Y.; Kobayashi, K.; Migita, C. T.; Elias, M. D.; Nakamura, S.; Tagawa, S.; Yamada, M. *J. Biol. Chem.* **2008**, *283*, 22215–22221.

(27) (a) Seki, S.; Yoshida, Y.; Tagawa, S.; Asai, K. *Macromolecules* **1999**, *32*, 1080–1086. (b) Seki, S.; Koizumi, Y.; Kawaguchi, T.; Habara, H.; Tagawa, S. *J. Am. Chem. Soc.* **2004**, *126*, 3521–3528.

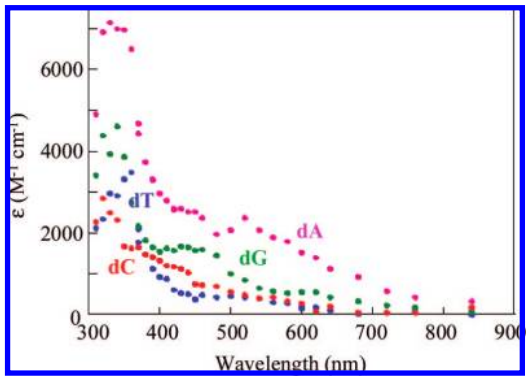

Figure 1. Absorption spectra at 200 ns after pulse radiolysis of Ar-saturated aqueous solutions at pH 7.0 containing 0.1 M *tert*-butyl alcohol, 20 mM phosphate buffer, and 10 mM of each nucleotide, dA, dC, dT, or dG (5 mM).

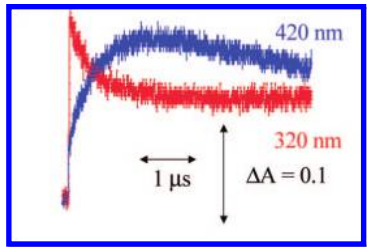

Figure 2. Absorbance changes after pulse radiolysis of a solution containing 20 mM dT and 0.5 mM *N*-methylnicotinamide. Experimental conditions were the same as those described in the legends for Figure 1 .

transported the electron pulse-induced transmittance changes to a gated spectrometer (Unisoku, TSP-601-02).[21,26e]

Radiation chemical dosimetry was performed with the KSCN system by measuring the optical density due to $\epsilon(SCN)_2^{-\bullet}$ at 480 nm (7600 M^{-1} cm^{-1}).[22] The extinction coefficients were determined by the absorbance changes at 420 nm due to electron transfer from electron adducts of deoxynucleotides to *N*-methylnicotinamide (NMA).[28] The concentrations of deoxynucleotides and NMA were 5−10 and 0.5−1 mM, respectively.

Optical absorption spectra were measured using a Hitachi U-3000 spectrometer with temperature control.

Results

Electron Adduct of Deoxynucleotides. Electron adducts of nucleotides were produced by pulse radiolysis of a deaerated aqueous solution of dA, dG, dC, or dT 5−10 mM and *tert*-butyl alcohol 0.1 M to scavenge OH radicals. Under these conditions, a hydrated electron (e_{aq}^-) reacts with the nucleotides within 10 ns, assuming that the rate constants of e_{aq}^- with the nucleotides were $\sim 10^{10}$ M^{-1} s^{-1}.[22−24] The absorption spectra recorded after complete decay of e_{aq}^- are shown in Figure 1. These spectra are essentially similar to those reported previously, although we observed small differences at longer wavelengths (>500 nm). Each extinction coefficient (ϵ) could be determined by the charge-transfer reaction between the electron adduct of each nucleotide and NMA. A typical example is shown in Figure 2. The formation of the electron adduct of dT was complete within <50 ns, and its decay at 320 nm was due to transfer of an electron to NMA. The formation of the NMA radical could be observed as an increase in the transient absorption at 420 nm, the wavelength at which the NMA radical has an extinction coefficient of 4300 cm^{-1} M^{-1}.[28] The extinction coefficients of pyridium-derived electron adducts were less than those of purine derivatives.

The protonation and deprotonation of pyrimidine radical anions $T^{\bullet-}$ and $C^{\bullet-}$ have been regarded as important for electron hopping through DNA duplexes.[7d,10−13] Below pH 7, following the spectral changes due to the reaction of e_{aq}^- with dT, other spectral changes occurred in the time range of nanoseconds. A typical absorbance change at 350 nm is shown in Figure 3A. Above pH 7, the absorbance at 350 nm was unchanged (Figure 3B). Figure 4 shows the spectra recorded at 1 μs after the pulse at pH 3.5, 7.0, and 10.5. To confirm the pH-dependence of the spectra, absorbance changes after the pulse were plotted against pH (Figure 5). These changes fit well to a p*K* profile with an inflection point at 6.8, which is similar to the p*K* value 6.9 determined by kinetic measurement.[22] Therefore, the spectra at pH 3.5 and 10.5 can be identified as those of $T(H)^{\bullet}$ and $T^{\bullet-}$, respectively. These findings indicate that $T^{\bullet-}$ formed transiently within the pH range and that the change in absorbance shown in Figure 3A was due to the protonation of $T^{\bullet-}$ to $T(H)^{\bullet}$, as shown in eq 1.

$$T^{\bullet-} + H^+ \rightleftarrows T(H)^{\bullet} \qquad (1)$$

The apparent rate constant of the protonation at pH 7.0 was 4.3×10^5 s^{-1}. This rate constant was likely due to the direct combination of $T^{\bullet-}$ with solution protons, because the plot of the apparent first-order rate constant versus H^+ was linear (Figure 6). From the slope and intercept in Figure 6, the rate constants for protonation and deprotonation could be calculated as 1.8×10^{10} M^{-1} s^{-1} and 2.4×10^6 s^{-1}, respectively. The pH-dependent changes in the absorbance changes (Figure 5) and kinetic results (Figure 6) indicate that the change of $T^{\bullet-}$ was due to reversible protonation (reaction 2).[22]

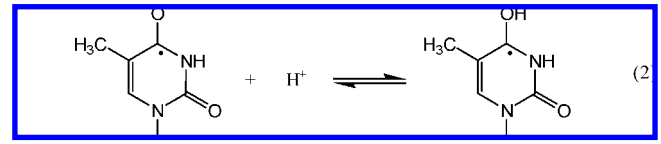

A similar experiment was performed using dC. We found the species with an absorption maximum at 425 nm did not change over the pH range 3.4−12.0 and decayed without any observable intermediates on a time scale of hundred of microseconds (data not shown). Conductance measurements have shown that the electron adduct of C is protonated at pH 6−10.6,[29] indicating that protonation occurs very rapidly and this process is complete within <20 ns.[9,13,29]

Electron Adduct of ODNs. A similar experiment was performed using a systematic series of double-stranded and single-stranded ODNs. We compared the kinetic difference spectra at 400 ns after pulse radiolysis of ODNs **GC** and **AT** with those of single-stranded ODNs and the isolated nucleotides (Figure 7). A control experiment using single-stranded ODNs showed that the transient spectra of the electron adducts of 5′-CGGCCCGGCGC-3′ (**GC**) and 5′-TAATTTAATAT-3′ (**AT**) were essentially similar to those of C and T, respectively, indicating that the electron adduct centers become localized mainly at C or T. An analogous situation exists for the di(2′-deoxy) nucleotide phosphates cytidylyl (3′→5′) deoxyguanosine CpdG) and dT and di(2′-deoxy) nucleotide phosphates thymidylyl (3′→5′) deoxyadenosine (TpdA) (data not shown). In these

(28) Kosower, E. M.; Swallow, A. J.; Land, E. J. *J. Am. Chem. Soc.* **1972**, *94*, 986–987.

(29) Hissung, A.; von Sonntag, C. *Int. J. Radiat. Biol.* **1979**, *35*, 449–458.

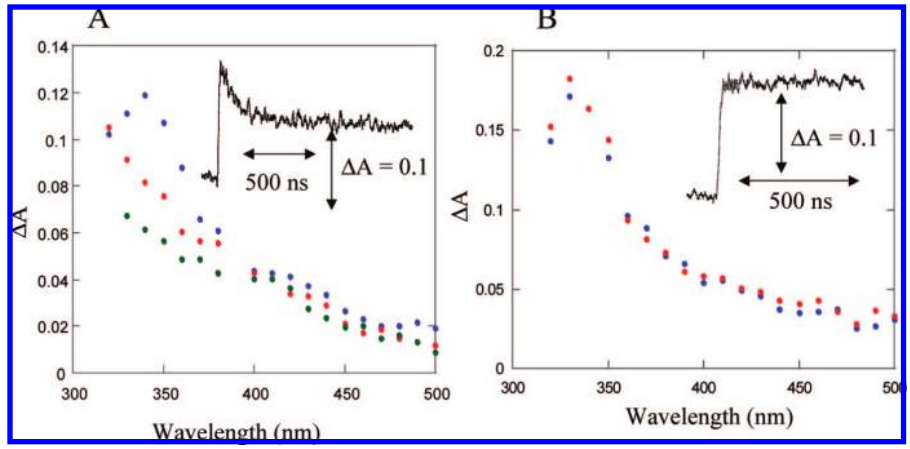

Figure 3. Kinetic difference spectra of pulse radiolysis of dT at 10 ns (blue), 100 ns (red), and 1 μs (green) at pH 3.5 (A) and 10.5 (B). Inset: Absorption changes at 350 nm after pulse radiolysis of dT.

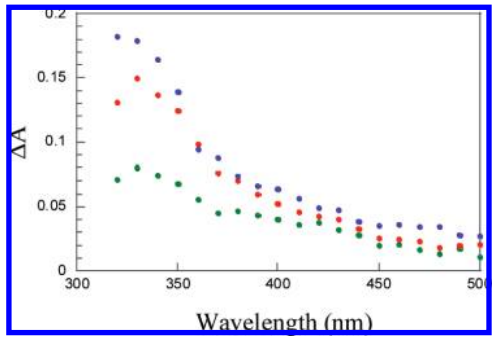

Figure 4. Kinetic difference spectra at 1 μs after pulse radiolysis of dT at pH 3.5 (green), pH 7.0 (red), and pH 10.5 (blue).

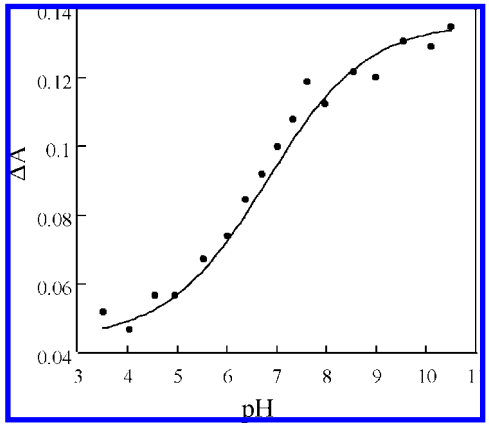

Figure 5. pH-dependence absorbance changes at 350 nm after pulse radiolysis of dT.

systems, electron transfer from the adducts initially formed at the C or T sites is completed within 10 ns.

The spectrum of double-stranded ODN **GC** has a broad absorption at 450 nm and longer wavelengths (>600 nm), whereas that of dC shifts slightly to a shorter wavelength (420 nm) and has no absorption at longer wavelengths. The transient spectrum of double-stranded **AT** has an absorption maximum at 480 nm and a broad absorption above 600 nm, which differs from that of the single-stranded ODN **AT**.

Following spectral change due to the reaction of e_{aq}^- with ODN **AT**, other spectral changes took place in the time range of microseconds. A typical change in absorbance at 350 nm is

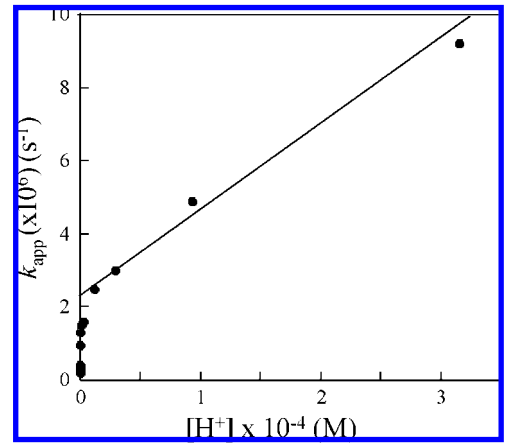

Figure 6. k_{app} vs pH plot in the protonation of $T^{-\bullet}$ determined at 350 nm.

shown in Figure 8. The decrease in absorbance fits well with an exponential curve, yielding a rate constant of 4×10^4 s^{-1}. Figure 8 shows the kinetic difference spectra after pulse radiolysis of ODN **AT**. The kinetic difference spectra for the subsequent process have an absorption maximum at 350 nm, indicating that spectroscopic change at 100 μs accounts for the protonation of $T^{\bullet-}$ in ODN. This species which is generated at 500 μs, similar to T, was stable, persisting for at least 2 s after pulse radiolysis.

Discussion

The results presented here strongly suggest that the transient spectra of the ODNs **GC** and **AT** correspond to the electron adducts of G−C and A−T base pairs in double-stranded DNA, not to the corresponding composite spectra of G plus C or A plus T. This is supported by the significant differences between the spectra of single-stranded and double-stranded ODNs. The spectra of the single-stranded ODNs primarily reflect the spectra of the one-electron reduced C and T moieties. An analogous situation was observed for CpdG and TpdA. In these systems, e_{aq}^- reacts with both bases unselectively, with subsequent electron transfer from $G^{-\bullet}$ to C or from $A^{-\bullet}$ to T occurring at millimolar concentrations of ODNs and the process driven by the redox potential of the bases.[18] In contrast, our findings suggest that the transient species generating the 200 ns spectra in the double-stranded ODN may be a resonance structure of

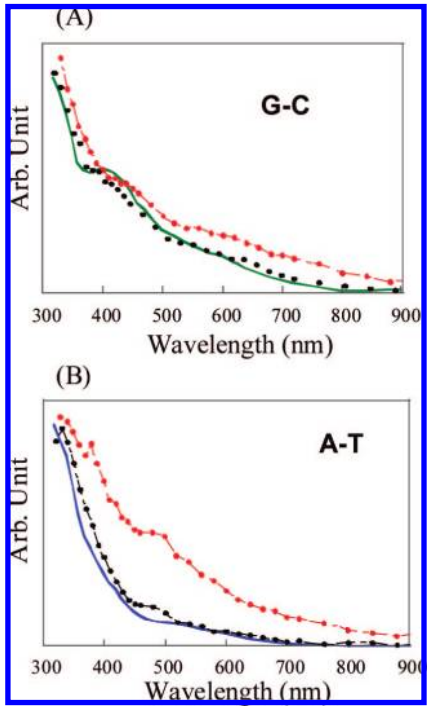

Figure 7. Kinetic difference spectra following pulse radiolysis of (A) double-stranded (red) and single-stranded **GC** (black) and dC green line, and of (B) double-stranded (red) and single-stranded (black) **AT** and dT blue line. Samples contained 3 mM ODNs, 0.1 M *tert*-butyl alcohol, and 20 mM phosphate buffer (pH 7.0). The spectra were taken 200 ns after pulse radiolysis.

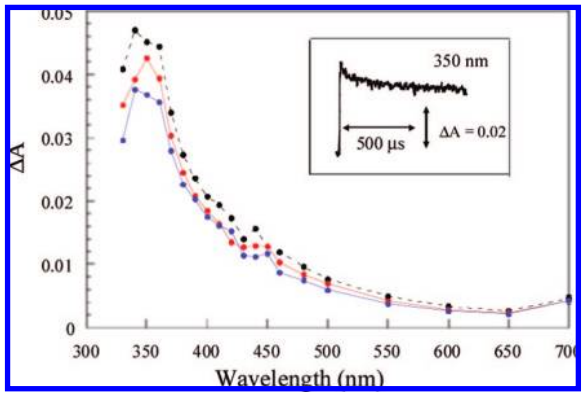

Figure 8. Kinetic difference spectra of pulse radiolysis of ODN **Pal AT** at 10 (black), 50 (red), and 150 μs (blue). Inset: Absorption changes at 350 nm after pulse radiolysis of ODN **Pal AT**.

$(G-C)^{-\bullet}$ and $(A-T)^{-\bullet}$. The spectra of excess electrons did not significantly differ from those of dC and dT. This result is consistent with theoretical calculations, in which the unpaired electrons of G−C[16e] and A−T[16c] base pairs are localized to C and T, respectively. However, the base pair intermediates of ODN AT is characterized by an absorption maximum at 480 nm and the broad absorption from 600 to 900 nm. In contrast, the corresponding single-stranded ODN AT and dT had no absorption in this range. The transiently formed electron adduct of T is stabilized by base pairing with A. Alternatively, it may be due to the spectral changes caused by the stacking interactions of neighboring nucleobases as observed in G cation radicals of ODNs.[21] Theoretical calculations show that the anion radicals of pyrimidines are strongly influenced by neighboring nucleobases and that 5′-TTT-3′ and 5′-TCT-3′ are the strongest electron sinks.[30] An alternative theoretical calculation showed that excess electrons in DNA are confined to a single pyrimidine, not localized over several nucleobases.[17] In the present experiment, however, the spectra were due to the excess electrons of C in GC and CC or T in TT and AT. We are currently investigating the dynamics of excess electrons using a systematic series of ODNs.

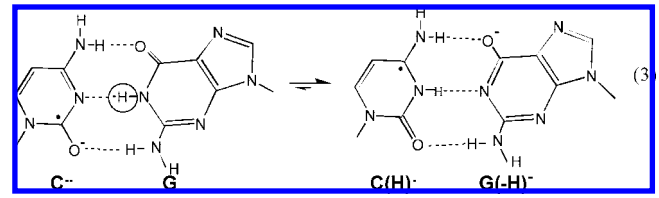

(3)

Proton-transfer reactions are important for the stabilization of initial DNA ion radicals.[1,21−23,25,31] In regard to excess electrons of DNA, attention has focused on the protonation state and protonation sites of C and T. In the G−C pair, $\mathbf{C}^{-\bullet}$ rapidly acquires a proton at N3 through hydrogen bonding with the HN1 of G. From the pK_a values of the N3 protonated $\mathbf{C(H)}^{\bullet}$ (pK_a > 13) and the N1 proton of G (pK_a = 9.5),[22] the equilibrium constant for the proton transfer is estimated to be 3.16×10^3. Therefore, as shown in eq 3, the equilibrium of $\mathbf{GC}^{\bullet-}$ in ODN **GC** is far to the right, and the spectrum shown in Figure 7A is regarded as corresponding to $\mathbf{G(-H)}^{-}\mathbf{-C(H)}^{\bullet}$. Theoretical calculations also indicate that transfer of the central proton in the G−C base pair anion radical is energetically favorable with a small activation energy.[6f] Moreover, the protonation of free dC occurs before 10 ns. Such a rapid reaction may be due to protonation by water-bound N3 of C. Similar results were observed using conductance techniques,[29] and in ESR/ENDOR studies of cytosine monohydrate single crystals irradiated at 10 K.[32] In contrast, since $T^{-\bullet}$ is only a weak base, it was present transiently in a neutral aqueous solution and protonated to form the neutral radical $T(H)^{\bullet}$ in the time range of microseconds. The resulting products of dT decayed without any observable intermediates (data not shown). Under our experimental conditions, $T(H)^{\bullet}$ is a protonation species of $T^{-\bullet}$, whereas another chemical species, resulting from protonation at C6, appeared after the reaction of e_{aq}^{-} with uracil at high buffer concentration.[33] Thus, protonation of dT occurs reversibly at O4 by the direct combination of $T^{-\bullet}$ with protons in solution. This is consistent with studies of anhydrous thymine single crystals irradiated at 10 K, in which the primary reduction product was an O4-protonated thymine anion.[34] In double-stranded ODNs, since the pK_a values of the O4 of protonated $T(H)^{\bullet}$ (pK_a = 6.9) and the N6 of A (pK_a > 13.75),[22] $T^{-\bullet}$ is not be protonated by its complementary base, A. Thus, the spectrum of the electron adduct of ODN **AT** in Figure 7B corresponds to $A-T^{\bullet-}$. The process of the protonation of T in ODN **AT** is thus consistent with a slower process spectroscopic change observed on a scale of hundreds of microseconds. Remarkably, however, this process revealed a substantial difference between the ODN **AT** and free

(30) Voityuk, A. A.; Michel-Beyerle, M.-E.; Rosch, N. *Chem. Phys. Lett.* **2001**, *342*, 231–238.
(31) Bernhard, W. A. *Adv. Radiat. Biol.* **1981**, *9*, 199–280.
(32) Sagstuen, E.; Hole, E. O.; Nelson, W. H.; Close, D. M. *J. Phys. Chem.* **1992**, *96*, 8269–8276.
(33) (a) Hole, E. O.; Sagstuen, E.; Nelson, W. H.; Close, D. M. *J. Phys. Chem.* **1991**, *95*, 1494–1503. (b) Sagstuen, E.; Hole, E. O.; Nelson, W. H.; Close, D. M. *J. Phys. Chem.* **1992**, *96*, 1121–112.
(34) Das, S.; Deeble, D. J.; Schuchmann, M-N.; Von Sonntag, C. *Int. J. Radiat. Biol.* **1984**, *46*, 7–9.

dT. At pH 7.0, the rate constant of the former (4×10^4 s^{-1}) was 10-fold slower than that of the latter (4.3×10^5 s^{-1}). In addition, the rates of ODN **AT** were independent of the change in pH from 5.8 to 8.3. This difference may be due to the differences in the protonation sites of T in DNA and free dT. ESR studies using low-temperature glasses yielded strong evidence that when DNA was exposed to ionizing radiation at 77 K, an ESR doublet associated with $T^{-\bullet}$ was converted into a readily identifiable eight-line spectrum of the 5,6-dihydrothymine-5-yl radical,[6a,e,35] a conversion due to the irreversible protonation of $T^{\bullet-}$ at C6. A water molecule bound to DNA would participate in this protonation. Thus, irreversible protonation by water at C6 is both pH-independent and relatively slower.

Our results have important implication for electron transport through DNA. Recently, electron transport in DNA was shown to proceed similarly to hole migration.[36,37] Both hole and electron transport display a shallow dependence on distance and perturbation in the intervening base stack significantly altering the efficiency of transfer. Thus, the electron transfer along DNA would occur in the time range 10^6-10^{10} s^{-1}, as does hole transfer. Transfer rates decrease as distance increases, and transfer competes with the protonation of $T^{\bullet-}$ and $C^{-\bullet}$. The long-distance migration is possible in the microsecond time scale. Our results show that the protonation of $C^{-\bullet}$ in DNA occurs very rapidly, suggesting that long-range electron migration is unlikely, once an electron has localized on the C residue, consistent with results showing that the G−C base pair inhibits the efficiency of electron transfer. In contrast, protonation of thymine occurs on a 100-μs time scale, suggesting that the electron transfer along DNA in this time range occurs prior to the protonation of $T^{\bullet-}$.Thus, the rate of electron transfer should be greater than 10^4 s^{-1}, making long-range electron transfer possible across the intervening A−T bridge.

Conclusions

We observed spectrophotometrically that electron adducts of G−C and A−T in double-stranded DNA were formed transiently. Subsequent absorbance changes due to the protonation of T in ODNs were detected on a time scale of microseconds. In contrast, unprotonated $dC^{\bullet-}$ was not a stable intermediate in water, both isolated nucleobases, and DNA.

Acknowledgment. We thank members of the Radiation Laboratory of the Institute of Scientific and Industrial Research, Osaka University, for their assistance in operating the accelerator. We thank Drs. Shu Seki and Masakazu Okamoto of the Institute of Scientific and Industrial Research, Osaka University, for experimental support, and we thank Dr. Kiyohiko Kawai of the Institute of Scientific and Industrial Research, Osaka University, for valuable advice and helpful discussions.

JA805127E

(35) Ormerod, M. G. *Int. J. Radiat. Biol.* **1965**, *9*, 291–300.
(36) Elias, B.; Shao, F.; Barton, J. K. *J. Am. Chem. Soc.* **2008**, *130*, 1152–1153.
(37) Valis, L.; Wang, Q.; Raytchev, M.; Buchvarov, I.; Wagenknecht, H. A.; Fiebig, T. *Proc. Natl. Acad. Sci. U.S.A.* **2006**, *103*, 10192–10195.